$\kappa^2-\kappa^3$ Isomerism in Rhodium(I) Tris(pyrazolyl)borate Complexes of the Type $Tp^{3R,4R,5R}Rh(LL)$ (LL = 2 CO, COD, and NBD) and Their Dynamic Behavior in Solution. X-ray Crystal Structure of $Tp^{Me}Rh(NBD)$

Urs E. Bucher, Antonio Currao, Reinhard Nesper, Heinz Rüegger, Luigi M. Venanzi,* and Elizabeth Younger

Laboratorium für Anorganische Chemie, Eidgenössische Technische Hochschule, Universitätsstrasse 6, CH-8092 Zürich, Switzerland

Received February 25, 1994[⊗]

Rhodium(I) complexes of the type $Tp^{3R,4R,5R}Rh(LL)$ (LL = 2 CO, NBD (norbornadiene), COD (1,5-cyclooctadiene), 3R = 4R = 5R = H; 3R = Me, 4R = 5R = H; 3R = Me, Ph, CF_3, 4R = H, 5R = Me; 3R = Me, 4R = Me, Cl, 5R = Me; 3R = ^iPr, 4R = Br, 5R = H) were synthesized and fully characterized. Isomeric forms of three types were identified in solution for these compounds: type **A**, square planar complexes in which the $Rh(NN)_2B$ six-membered ring has a boat conformation, the third pyrazolyl ring being free and occupying an equatorial position; type **B**, compounds with a coordination geometry and chelate ring as above, but having the third pyrazolyl ring in an axial position, i.e., an arrangement which can easily form penta-coordinate complexes; type **C**, five-coordinate species which, however, on the NMR time scale, are in a fast exchange with those of type **B**. In the carbonyl complexes (LL = 2 CO), compounds of type **C** can be distinguished from the forms **A** and **B** by IR spectroscopy. The dynamic equilibria between the corresponding isomeric structures, **A**, **B**, and **C**, are solvent-dependent and can be shifted completely toward the forms **B** and **C** by placing a methyl substituent in the 5-position of each pyrazole. For compounds possessing COD as a co-ligand, the formation of square-planar complexes of type **B**, with κ^2-bonded pyrazolylborates is preferred, as indicated by ^{103}Rh NMR spectroscopy, whereas both four- and five-coordinate species are present in compounds having NBD as a co-ligand, their relative contributions being dependent on the substituents on the pyrazolyl rings. The X-ray crystal structure of the compound $Tp^{Me}Rh(NBD)$ (space group $P2_1/c$, a = 18.152(3), b = 16.732(4), c = 20.591(4) Å; β = 141.793(7); Z = 8; R = 0.0457, R_w = 0.0412 for 3904 observed reflections) shows that the tris(pyrazolyl)borate ligand is κ^3-bonded and the rhodium atom has a distorted trigonal bipyramidal structure (type **C**), the two olefinic double bonds being in an equatorial and an axial position, respectively.

Introduction

Pyrazolylborate anions of the type $[H_{4-n}B(pz)_n]^-$ (pz = pyrazolyl, n = 2−4), and their coordination compounds have been widely used in organometallic chemistry since Trofimenko's original publication,[1] as the steric and electronic properties of these ligands are easily modified by changing the number of pyrazolyl rings and the substituents thereon or at the boron center.[2] The tris(pyrazolyl)borates, the class most often employed, are potentially tridentate ligands and, normally, coordinate facially in a tripodal fashion. However, the denticity of poly(pyrazolyl)borate ligands can often differ from n, being, e.g., n − 1 for κ^2-bonded tris(pyrazolyl)borates, or n + 1 for some types of bis-pyrazolylborates through participation of side chains in, e.g., agostic bonding.[3]

Variations of poly-pyrazolylborate denticity can easily occur in Rh(I) and Ir(I) complexes which may exist either as $16e^-$ or $18e^-$ species. Thus, the compounds pzTpRh(LL) were shown[4] to exist in the solid state as $16e^-$−κ^2 complexes when LL was NBD and COD and as an $18e^-$−κ^3 species when LL was duroquinone. However, all three compounds were assigned five-coordination in solution.[5] $\kappa^2-\kappa^3$ isomerism has also been postulated[6] for the carbonyl complex $Tp^{Me2}Rh(CO)_2$, whereas analogous isonitrile compounds, in solution as well as in the solid state, have been reported to contain κ^2-bonded tris(pyrazolyl)borate ligands.[7]

As a contribution to the fast developing chemistry of transition metals with poly(pyrazolyl)borate compounds, this paper describes Rh(I) complexes containing a variety of substituted tris(pyrazolyl)borates. These compounds were characterized by IR and multinuclear NMR methods and, for $Tp^{Me}Rh(NBD)$, by X-ray diffraction. Furthermore, aspects relating in particular to $\kappa^3-\kappa^2$ isomerism, its solvent dependence, and the dynamic processes occurring in solution, as evidenced by IR and one- and two-dimensional NMR spectroscopy, have been investigated.

Results

1. Synthesis. The tris(1-pyrazolyl)borate anions $[Tp^{3R,4R,5R}]^-$, as their sodium or potassium salts, react with the rhodium complexes $Rh_2Cl_2(LL)_2$ (LL = 2 CO, NBD, COD), in dry MeCN, according to eq 1. The products are yellow to orange

[⊗] Abstract published in *Advance ACS Abstracts,* November 15, 1994.

(1) Trofimenko, S. *J. Am. Chem. Soc.* **1966**, *88*, 1842.
(2) (a) Trofimenko, S. *Chem. Rev.* **1993**, *93*, 943. The nomenclature for tris(pyrazolyl)borate ligands and their complexes, as proposed by S. Trofimenko herein, is used throughout this publication. (b) Trofimenko, S. *Prog. Inorg. Chem.* **1986**, *34*, 115.
(3) Trofimenko, S.; Calabrese, J. C.; Thompson, J. S. *Inorg. Chem.* **1992**, *31*, 974.
(4) Cocivera, M.; Ferguson, G.; Kaitner, B.; Lalor, F. J.; O'Sullivan, D. J.; Parvez, M.; Ruhl, B. *Organometallics* **1982**, *1*, 1132.
(5) Cocivera, M.; Ferguson, G.; Lalor, F. J.; Szczecinski, P. *Organometallics* **1982**, *1*, 1139.
(6) Ball, R. G.; Ghosh, C. K.; Hoyano, J. K.; McMaster, A. D.; Graham, W. A. G. *J. Chem. Soc., Chem. Commun.* **1989**, 341.
(7) Jones, W. D.; Hessell, E. T. *Inorg. Chem.* **1991**, *30*, 778.

0020-1669/95/1334-0066$09.00/0

$$Rh_2Cl_2(LL)_2 + 2\ Na[Tp^{3R,4R,5R}] \xrightarrow{MeCN} 2\ Tp^{3R,4R,5R}Rh(LL) + 2\ NaCl \quad (1)$$

#	LL	3R	4R	5R
1	2 CO	Me	H	H
2	2 CO	Me	H	Me
3	2 CO	^{i}Pr	Br	H
4	NBD	Me	H	H
5	NBD	Me	H	Me
6	NBD	^{i}Pr	Br	H
7	COD	Me	H	H
8	COD	Me	H	Me
9	COD	^{i}Pr	Br	H
10	COD	Me	Me	Me
11	COD	Me	Cl	Me
12	COD	Ph	H	Me
13	COD	CF_3	H	Me
14	COD	H	H	H

air-stable solids. They are quite soluble in CH_2Cl_2 and $CHCl_3$, moderatly soluble in MeCN and hexane, and sparingly soluble in MeOH.

2. Carbonyl-Compounds 1−3. The ^1H and ^{13}C NMR spectra, recorded at room temperature in $CDCl_3$ and CD_3CN, for $Tp^{Me}Rh(CO)_2$ (**1**) and $Tp^{Me2}Rh(CO)_2$ (**2**) showed that, in both solvents, the three pyrazolyl rings were equivalent. This observation is consistent with the formation of five-coordinate complexes of type **C**, which then undergo fast intramolecular rearrangement rendering all nitrogen donors equivalent, or four-coordinate complexes of type **B** with fast exchange of coordinated and uncoordinated pyrazolyl rings.

The complex $Tp^{iPr,4Br}Rh(CO)_2$ (**3**), in CD_3CN, behaved analogously to **1** and **2** exhibiting only the species with dynamically averaged pyrazolyl rings (**B/C**). However, in $CDCl_3$, two species were identified, one having equivalent pyrazolyl rings, as found for **1** and **2**, and the other having two equivalent pyrazolyl rings, different from the third. The latter species is formulated as a complex of type **A** having the potentially tridentate ligand coordinated in a κ^2-fashion. A two-dimensional exchange spectrum, recorded in $CDCl_3$, indicated that the hydrogens on the three types of rings interchange slowly, pointing to a dynamic equilibrium between isomeric species. This equilibrium appears to be dependent on the polarity of the solvent used, shifting towards the **B/C** species in solvents having high dipole moments. The relative abundance of this form, determined by integration of the proton spectra, was found to increase from 45% in $CDCl_3$ to 56% in CD_2Cl_2, and 83% in acetone-d_6 being 100% in CD_3CN and DMSO-d_6. The positions of these equilibria did not change significantly on cooling the solutions to −60 °C.

Low-temperature experiments were also performed on $Tp^{Me}Rh(CO)_2$ (**1**) and $Tp^{Me2}Rh(CO)_2$ (**2**), in CD_2Cl_2. Compound **2**, showing, at room temperature, only the structure with dynamically averaged pyrazole rings, exhibited no change in its signal pattern even at −80 °C; whereas for **1** the component having the κ^2-structure of type **A** appeared at −65 °C, the latter isomer having an abundance of approximately 9% under these conditions.

At this point one could ask the question whether the species with apparently equivalent pyrazole rings are really five-coordinate, i.e., with κ^3-bonded tris(pyrazolyl)borates, or are instead four-coordinate complexes with fast exchange between coordinated and free pyrazolyl rings. This point will be discussed after presenting the results of some infrared spectroscopic studies, a technique having a more suitable time scale for this type of problem.

The ν(CO) stretching vibrations (sym and asym) of the carbonyl derivatives **1**−**3** are given in Table 1, together with the corresponding values for some complexes with bis(pyrazolyl)borates, and some representative IR spectra are shown in Figure 1.

The spectrum of $Tp^{iPr,4Br}Rh(CO)_2$ (**3**), in $CHCl_3$, showed two pairs of bands in the region 1900−2200 cm^{-1} (see Figure 1a), three of them being easily recognizable and the fourth appearing as a shoulder on the low-energy side of the band at 2026 cm^{-1}. Their energies are in the range characteristic for four-coordinate rhodium complexes, as can be seen by comparing these values with those of the corresponding bis(pyrazolyl)borate complexes given in Table 1. These results are consistent with the presence, in solution, of two different stereoisomers of **3**, *both* of them having *square-planar coordination geometries*. The intensity ratios of the IR bands are about the same as those of the two isomers observed by NMR spectroscopy. Therefore, the observed equivalence of pyrazole rings in the spectrum of one of the species arises from a dynamic phenomenon, i.e. fast exchange, on the NMR time-scale, between free and coordinated pyrazolyl groups, rather than from high molecular symmetry.

The complex $Tp^{Me2}Rh(CO)_2$ (**2**), in $CHCl_3$, has completely different IR absorption characteristics (see Figure 1b): The CO stretching bands are shifted to lower energy. Complex **2** is formulated as a five-coordinate species with a genuine κ^3-bonded tris-pyrazolylborate as it can be expected that the higher electron density at the 18-electron metal center will favor π-back-bonding and, therefore, bands at lower energies.

$Tp^{Me}Rh(CO)_2$ (**1**), in $CHCl_3$, showed a spectrum different from **2** or **3**, i.e., exhibiting absorptions for both types of complexes (Figure 1c). Furthermore, it shows a remarkable shift toward the five-coordinate form on replacing $CHCl_3$ by MeCN. However, there is no straightforward relationship between the relative intensities found by IR and NMR spec-

Table 1. Carbonyl Stretching Bands for Complexes of the Type $Tp^{3R,4R,5R}Rh(CO)_2$ and Related Compounds

	compound	$CHCl_3$		MeCN		RbI or KBr	
		ν_{sym}	ν_{asym}	ν_{sym}	ν_{asym}	ν_{sym}	ν_{asym}
1	$Tp^{Me}Rh(CO)_2$	2085 s	2019 s	2087 w	2019 w		
		2060 s	1988 s	2062 vs	1988 vs	2061	1981
2	$Tp^{Me2}Rh(CO)_2$	2055 vs	1980 vs	2056 vs	1980 vs	2052	1974
3	$Tp^{iPr,4Br}Rh(CO)_2$	2089 vs	2026 vs	2090 vs	2026 vs		
		2077 m	2020 m (sh)				
	$\{Ph_2B(pz)_2\}Rh(CO)_2$[a]					2074	2013
	$\{BBN(pz)_2\}Rh(CO)_2$[a]					2075	2013
	$\{BBN(3\text{-}Me\text{-}pz)_2\}Rh(CO)_2$[a]					2080	2015

[a] See ref 4; BBN = 9-borabicyclononane.

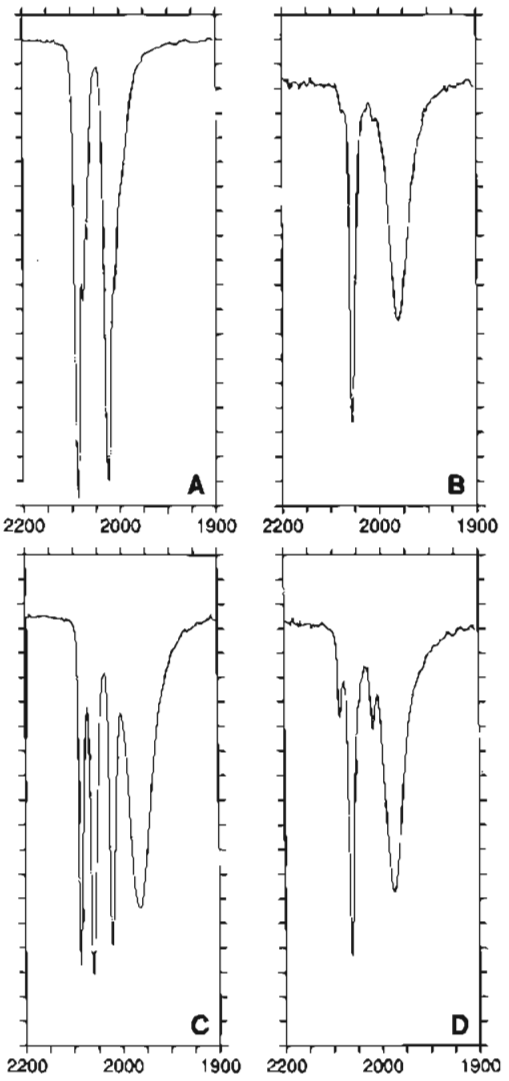

Figure 1. Infrared spectra showing the carbonyl stretching modes of (a) $Tp^{iPr,4Br}Rh(CO)_2$ (**3**) in $CHCl_3$, (b) $Tp^{Me2}Rh(CO)_2$ (**2**) in $CHCl_3$, and $Tp^{Me}Rh(CO)_2$ (**1**) in (c) $CHCl_3$ and (d) MeCN.

troscopic methods when one assumes that only two isomers are present. Therefore, it is proposed that the three isomers shown schematically in Figure 2 are present.

On one hand, the two square-planar forms (**A** and **B**) have (nearly) overlapping CO stretches at approximately 2080 and 2020 cm^{-1}, in agreement with values for derivatives having bis(pyrazolyl)borates as ligands, while form **C** absorbs at ca. 2060 and 1980 cm^{-1}. Thus the latter form can be distinguished from the other two by IR spectroscopy. On the other hand, form **A** can be distinguished from **B** and **C** by NMR spectroscopy, as the latter two give rise only to one set of resonances due to their fast mutual exchange on the NMR time scale.

The situation in the solid state appears to be slightly different from that in solution in that both $Tp^{Me}Rh(CO)_2$ (**1**) and $Tp^{Me2}Rh(CO)_2$ (**2**) show only the carbonyl stretches characteristic of the pentacoordinate forms.

3. Norbornadiene and Cyclooctadiene Compounds, 4–14. In view of the interesting solution properties of the carbonyl compounds discussed above and the possible structural differences between solids and solutions, the corresponding NBD and COD derivatives **4–14** were also prepared. The X-ray crystal structure of **4** was also determined. This will be discussed first.

X-ray Diffraction Study. The complex $Tp^{Me}Rh(NBD)$ (**4**) crystallizes as individual molecules separated by normal van der Waals distances. There are two crystallographically inde-

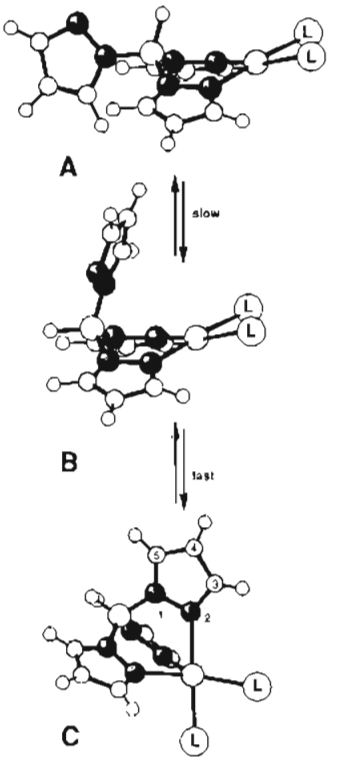

Figure 2. Proposed low-energy structures for isomer forms **A**, **B**, and **C** of complexes of the type TpRh(LL).

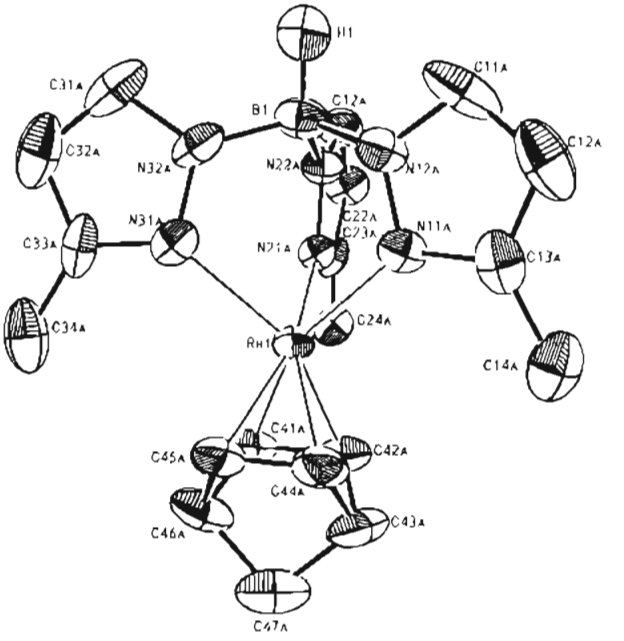

Figure 3. ORTEP view of the molecule $Tp^{Me}Rh(NBD)$ (**4**).

pendent molecules in the asymmetric unit, which, however, have to be considered as being equal within the standard deviations. An ORTEP view of **4** is given in Figure 3, and a selection of interatomic distances and bond angles is presented in Table 2.

The rhodium center adopts a distorted trigonal bipyramidal coordination where the tris(pyrazolyl)borate ligand coordinates in a tripodal fashion, occupying one axial and two equatorial coordination sites. The Rh–N separation for the axially coordinated pyrazolyl ring (2.147(7) Å) is significantly shorter than those of the equatorially coordinated rings (average 2.25(1) Å). The NBD double bond occupying the axial position is significantly further away from rhodium ($Rh-m_{2a}$ = 2.05(1) Å) than that in the equatorial position ($Rh-m_{1a}$ = 1.95(1) Å).

Table 2. Selected Bond Distances (Å) and Bond Angles (deg) for $Tp^{Me}Rh(NBD)$ (**4**) (Esd's in Parentheses)[a]

	Bond Distances		
Rh−N11	2.247(9)	B−N12	1.51(2)
Rh−N21	2.147(7)	B−N22	1.56(2)
Rh−N31	2.25(1)	B−N32	1.52(3)
Rh−C41	2.07(1)	C41−C42	1.45(3)
Rh−C42	2.09(1)	C45−C44	1.37(3)
Rh−C44	2.154(8)	N11−N12	1.36(1)
Rh−C45	2.16(1)	N21−N22	1.40(1)
Rh−m_{1a}[b]	1.95(1)	N31−N32	1.39(1)
Rh−m_{2a}[b]	2.05(1)		
	Bond Angles		
N11−Rh−N31	89.6(4)	N21−Rh−C41	102.4(3)
N11−Rh−N21	82.2(3)	N21−Rh−C42	101.4(4)
N21−Rh−N31	82.4(4)	N21−Rh−C44	160.0(6)
N11−Rh−m_{1a}	137.0(3)	N21−Rh−C45	160.9(4)
N11−Rh−m_{2a}	102.1(2)	N31−Rh−C41	113.0(6)
N21−Rh−m_{1a}	102.7(2)	N31−Rh−C42	153.7(5)
N21−Rh−m_{2a}	173.6(2)	N31−Rh−C44	115.7(5)
C41−Rh−C42	40.7(7)	N31−Rh−C45	88.2(5)
C44−Rh−C45	37.0(6)	N32−B−N22	108(1)

[a] Mean values for the two crystallographically independent molecules are given. [b] m_{1a} = $^1/_2$(C41−C42) and m_{2a} = $^1/_2$(C44−C45).

It is also possible that the axial double bond is shorter (1.37(3) Å) than the equatorial (1.45(3) Å), in agreement with the expectation of better π-back-bonding in the equatorial positions of a trigonal-bipyramid. All of the above-mentioned structural features for **4** are also found in the analogous B−Me substituted complex $MeTp^{Me}Rh(NBD)$,[8] and in the previously reported[4] related complex pzTpRh(duroquinone). It is noteworthy that the NBD and COD analogs of the latter compound were found to be square-planar with κ^2-bonded $B(pz)_4^-$ ligands. Thus, subtle electronic and steric differences, possibly even the crystal packing forces, may determine whether such Rh(I) poly(pyrazolyl)borate complexes occur as a four- or a five-coordinate species in the solid state.

NMR Solution Studies. The proton NMR spectra of $Tp^{Me2}Rh(COD)$ (**8**), $Tp^{Me3}Rh(COD)$ (**10**), $Tp^{Me2,4Cl}Rh(COD)$ (**11**), $Tp^{Ph,Me}Rh(COD)$ (**12**) and $Tp^{CF_3,Me}Rh(COD)$ (**13**), recorded in $CDCl_3$ solution at room temperature, indicated in each case the presence of only one type of molecule, i.e., that giving the spectrum showing dynamically averaged pyrazole rings, whereas for $Tp^{iPr,4Br}Rh(COD)$ (**9**), as well as for $Tp^{Me}Rh(COD)$ (**7**), two types of isomers could be recognized. In the latter compound, **7**, the structure assigned to types **B/C** predominates (70%), whereas the main isomer (75%) of **9** has been assigned a structure of type **A**.

As shown earlier for the carbonyl complexes, the appearance of magnetic equivalence in the ^1H and ^{13}C NMR spectra does not necessarely imply the presence of κ^3-bonded tris(pyrazolyl) ligands. While symmetry considerations in ^1H and ^{13}C NMR only allow for the indentification of complexes of type **A** in Figure 2, ^{103}Rh NMR parameters were considered for the differentiation between **B** and **C** in the expectation of large chemical shift variations between the 16e$^-$ and 18e$^-$ species. Relevant ^{103}Rh data are summarized in Table 3, and a typical example of a ^{103}Rh-^1H correlation spectrum is shown in Figure 4. Indirect detection[9,10] of ^{103}Rh resonances by ^1H observation was employed because it offers (i) significantly higher sensitivity compared to direct methods, (ii) a direct relation to the (easily interpretable) ^1H NMR spectrum, and (iii) insight into dynamic aspects related to reversible bond-breaking between the rhodium center and ligands.

Table 3. ^{103}Rh Chemical Shifts of Tris(pyrazolyl)borate Complexes of the Type $Tp^{3R,4R,5R}Rh(LL)$ and of Some Related Compounds[a]

			$\delta(^{103}Rh)$			
3R	4R	5R	compd	LL = COD	compd	LL = NBD
H	H	H	**14**	1253		
Me	H	H	**7**	1107,[b] 1106	**4**	1619
						1475[c]
Me	H	Me	**8**	1107	**5**	1777
Me	Me	Me	**10**	1110		
Me	Cl	Me	**11**	1101		
Ph	H	Me	**12**	1111		
CF_3	H	Me	**13**	1129		
^{i}Pr	Br	H	**9**	1130,[b] 1121	**6**	1274,[b] 1293
			15	1065[d]		
$\{Ph_2B(pz)_2\}Rh(LL)$				947		1034
$\{PhMeB(3\text{-}Me\text{-}pz)_2\}Rh(LL)$				1136		1340
$\{BBN(pz)_2\}Rh(LL)$						1097
$\{BBN(3\text{-}Me\text{-}pz)_2\}Rh(LL)$				1205[e]		1374

[a] Chemical shifts in $CDCl_3$ were measured indirectly by two-dimensional methods[9] and are expressed relative to the absolute scale Ξ = 3.16 MHz. [b] Isomer of type A. [c] $MeTp^{Me}Rh(NBD)$, see ref 8. [d] One of the pz-rings had undergone a 1,2-shift. [e] See ref 10.

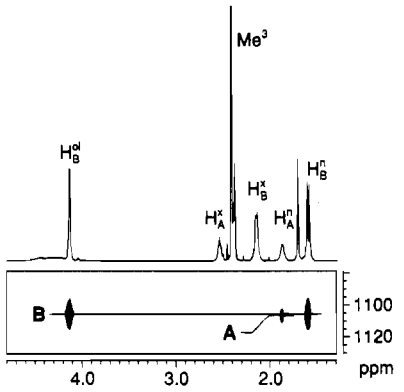

Figure 4. Section of the $^{103}Rh-^1H$ heteronuclear correlation spectrum showing the COD part for the two isomers of type **A** (minor) and **B** (major) of $Tp^{Me}Rh(COD)$ (**7**).

As shown by the data for the bis(pyrazolyl)borates given in Table 3, the $\delta(^{103}Rh)$ values of four-coordinate COD complexes fall between 947 and 1205 ppm while those for the NBD complexes are between 1034 and 1374. These can be taken as reference values for the 16e$^-$ complexes. Futhermore, a square-planar structure of type **A** has been assigned to the minor isomer of $Tp^{Me}Rh(COD)$ (**7**) on the basis of its ^1H and ^{13}C NMR characteristics, and its ^{103}Rh chemical shift (1107 ppm) is in the range expected for a complex of this type. Interestingly, the value for the other isomer with dynamically equivalent pyrazolyl rings, which is assigned structure **B**, is almost identical (1106 ppm), as are those of the complexes **8**−**13** showing equivalent pyrazolyl rings (1065−1130 ppm). It is, therefore, concluded that all these complexes exist in solution as their square-planar isomers (type **B**) with κ^2-bonded pyrazolylborates. The magnetic equivalence observed in their ^1H and ^{13}C NMR spectra can, once again, be explained by a fast exchange between coordinated and free pyrazolyl donors.

The only exception in the series of COD complexes is TpRh(COD) (**14**), i.e., the molecule with the unsubstituted pyrazolylborate ligand. A shift toward higher field of the ^{103}Rh resonance would be expected for this derivative should its

(8) Bucher, U. E.; Fässler, T. F.; Hunziker, M.; Nesper, R.; Rüegger, H.; Venanzi, L. M. *Gazz. Chim. Ital.*, in press.
(9) Benn, R.; Brenneke, H.; Rufinska, A. *J. Organomet. Chem.* **1987**, *320*, 115. Benn, R.; Brevard, C.; Rufinska, A.; Schroth, G. *Organometallics* **1987**, *6*, 938. Nanz, D.; von Philipsborn, W.; Bucher, U. E.; Venanzi, L. M. *Magn. Reson. Chem.* **1991**, *29*, S38. Imhof, D.; Rüegger, H.; Venanzi, L. M.; Ward, T. R. *Magn. Reson. Chem.* **1991**, *29*, S73.
(10) Bortolin, M.; Bucher, U. E.; Rüegger, H.; Venanzi, L. M.; Albinati, A.; Lianza, F.; Trofimenko, S. *Organometallics* **1992**, *11*, 2514.

structure be the same as for the other analogs. Generally, the replacement of a methyl substituent in 3-position of the pyrazolyl ring by hydrogen results in a high field displacement of the ^{103}Rh resonance as can be deduced, e.g., from the values of this parameter, 1097 and 1374 ppm, for {BBN(R^3-pz)$_2$Rh(NBD), where R^3 = H and Me, respectively, or the other data given in Tables 3 and 5. However, a shift in the opposite direction, i.e., toward lower field, is actually observed (δ(Rh) = 1253 ppm) and, therefore, this behavior can be taken as an indication for the formation (at least in part) of the five-coordinate complex **C**.

Of the complexes having NBD as co-ligand, only Tp^{iPr,4Br}Rh(NBD) (**6**) appears to form exclusively the two isomers with square-planar structures, while the low field shifts for Tp^{Me}Rh(NBD) (**4**) and Tp^{Me2}Rh(NBD) (**5**) indicate that five-coordinate forms of these complexes certainly exist in solution.

A special aspect related to the dynamic behavior, i.e., point iii above, should be mentioned: while coupling between the pyrazolyl ring protons and the rhodium spin is generally observed in the model complexes {Ph$_2$B(pz)$_2$}Rh(LL), {MePhB-{3-Mepz)$_2$}Rh(LL) and {BBN(pz)$_2$}Rh(LL) (LL = COD and NBD), such interactions are absent in the tris(pyrazolyl) complexes showing equivalent pyrazolyl rings, i.e, **4**−**14**. This points again to a fluxional process involving bond breaking between rhodium and the nitrogen donors, which is fast compared to the (small) magnitude of the coupling constants J(Rh,H^{pz}).

4. Additional NMR Studies. As demonstrated above, ^{103}Rh chemical shifts are sensitive NMR parameters for the evaluation of the equilibria between four- and five-coordinate rhodium(I) species. In cases where this parameter cannot be obtained, e.g. due to instrumental limitations or in the corresponding iridium complexes, the following alternative methods can be considered:

***(a)* ^{13}C Shift Data for the Olefinic Carbons.** Depending on the extent of π-back-bonding, olefin coordination can also be described, as limiting structure, in the canonical form of a metallacyclopropane. It is expected that this latter formulation is more appropriate for the five-coordinate complexes as the 18-electron system should show a higher π-back-bonding ability than the corresponding 16-electron systems. It is also expected that in such a metallaalkane the "organometallic" carbons are more shielded (smaller ^{13}C shifts). Values for this parameter are compiled in Table 4.

A chemical shift of ca. 80 ppm for the olefinic carbon resonance appears to be "normal" for four-coordinate Rh−COD complexes based on data for (1) the bis(pyrazolyl)borate model compounds, (2) the minor isomer of Tp^{Me}Rh(COD) (**7**), and (3) the two isomers of Tp^{iPr,4Br}Rh(COD) (**9**). On the other hand, the presumed five-coordinate TpRh(COD) (**14**) shows indeed a lower chemical shift (73.3 ppm) and that of Tp^{Me2}Rh(COD) (**8**) has an intermediate value (75.2 ppm).

Larger variations are observed for the complexes containing NBD as co-ligand. While the four-coordinate complexes containing bis-pyrazolylborates and Tp^{iPr,4Br}Rh(NBD) (**6**) have chemical shifts ranging from 51.0 to 57.6 ppm, significantly lower values are observed for Tp^{Me}Rh(NBD) (**4**) and Tp^{Me2}-Rh(COD) (**8**), 41.7 and 35.1 ppm, respectively, the latter complexes having been assigned five-coordinate structures in solution.

To support the postulate that a displacement of olefinic carbon resonances towards higher field is associated with the presence of five-coordinate complexes, the ^{13}C solid-state NMR spectrum of **4**, whose X-ray structure shows it to be trigonal-bipyramidal, was recorded. This spectrum, measured under cross-polarization and magic-angle spinning conditions, shows three groups of resonances in the 70−20 ppm range centered at δ = 58 ppm (bridges), 49 (bridgeheads), and 32 (olefinic). The shift spread for the group of olefinic resonances ranges from 30 to 35 ppm. Individual lines, corresponding to the anticipated eight olefinic signals for the two crystallographically independent molecules in the unit cell, are not resolved. However, their spectral positions strongly support the correlation outlined above.

Table 4. Selected ^{13}C, ^{15}N and ^{11}B NMR Data for Complexes of the Type Tp^{3R,4R,5R}Rh(LL), LL = COD, NBD[a]

	compound	^{13}C δ(olefinic)	^{15}N δ(N^1)	^{15}N δ(N^2)	^{11}B δ(B)	^{11}B T_1[b]
14	TpRh(COD)	73.3	−149.7	−122.2	−3.5	4.8
7	Tp^{Me}Rh(COD)	79.7			−2.0	3.5
8	Tp^{Me2}Rh(COD)	75.2			−6.0	2.9
9	Tp^{iPr,4Br}Rh(COD)	84.2, 78.0[c] 81.6			−2.2	1.8
	{BBN(pz)$_2$}Rh(COD)	81.1, 79.1	−131	−136		
	{BBN(3-Me-pz)$_2$}-Rh(COD)	78.3, 77.5				
4	Tp^{Me}Rh(NBD)	41.7			−3.1	4.3
5	Tp^{Me2}Rh(NBD)	35.1[d]			−9.3	3.2
6	Tp^{iPr,4Br}Rh(NBD)	57.6 57[c]			−2.3	1.9
	{BBN(pz)$_2$}(NBD)	54.7, 52.8				
	{BBN(3-Me-pz)$_2$}-Rh(NBD)	53.5, 51.0				
	Na[Tp][e]		−141.6	−71.3		
	K[BBN(pz)$_2$][e]		−135	−84		

[a] Recorded at 11.7 T, room temperature, $CDCl_3$. [b] Values from single exponential fit (ms). [c] Isomer of type A. [d] Solid state: 30−35 ppm. [e] DMSO-d_6.

***(b)* ^{15}N Shift Data for the Nitrogen Donors.** In free pyrazolylborates, the nitrogen chemical shifts of N^2, which are mainly determined by the low-lying n-π^* electronic transitions, have values which are *ca.* 50−70 ppm higher than those of N^1 (see Table 4). This difference decreases on coordination, and e.g., for the complex {BBN(pz)$_2$}Rh(COD), the N^2 resonance is found 5 ppm upfield from N^1; i.e., the coordination chemical shift of N^2 is −52 ppm while that of N^1 is +4 ppm.

In the experimental setup employed for this study, the nitrogen shift parameters are obtained indirectly from ^{15}N−^{1}H correlations which rely on suitable heteronuclear long-range coupling constants. Unfortunately, only the N^1 nucleus appears to couple to protons in all ring positions whereas N^2 couples only geminally to H^3. Thus at present its use is limited to unsubstituted pyrazolyl rings.

Of the rhodium tris(pyrazolyl)borate compounds described here, only TpRh(COD) (**14**) could be investigated and its N^2 resonance showed a coordination chemical shift of −50.9 ppm. Although it seems presumptuous to draw conclusions given the extremely limited set of data, it should be noted that this value is close to that of the reference material {BBN(pz)$_2$}Rh(COD) (52 ppm), suggesting that all nitrogen donors in **14** are coordinated; i.e., it is of type **C**.

***(c)* ^{11}B Longitudinal Relaxation Data.** The longitudinal relaxation rates of the quadrupolar boron spin are expected to be dominated by its interaction with the electric field gradient at the nucleus. This interaction being, among other factors, a function of local symmetry, is assumed to be stronger for complexes with square-planar geometry, than for the five-coordinate species where the local environment approaches axial symmetry, leading to shorter relaxation times in the former case. Indeed, the T_1 values appear to be structure sensitive, as they vary from 1.8 to 4.8 ms (see Table 4). The longest value has been observed for the unsubstituted pyrazolylborate in the complex TpRh(COD) (**14**). Furthermore the NBD complexes,

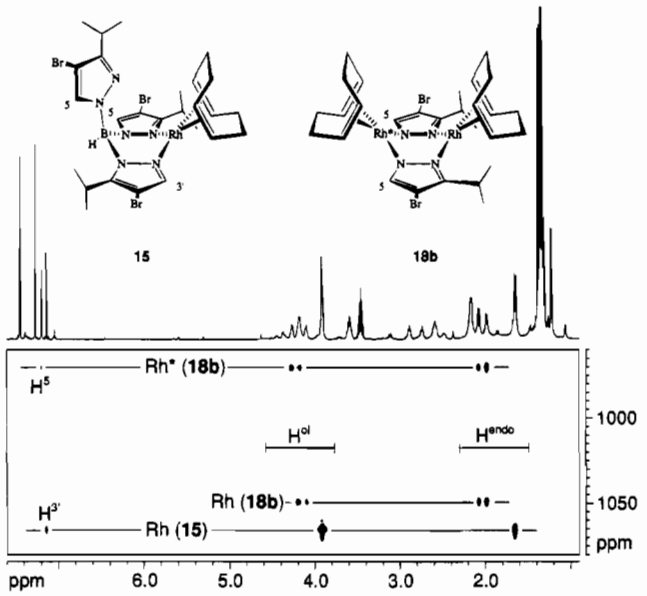

Figure 5. $^{103}Rh-^{1}H$ heteronuclear correlation spectrum showing a mixture of the two isomeric forms of $Rh_2\{3\text{-}^{i}Pr\text{-}4\text{-}Br\text{-}pz\}_2(COD)_2$ (**18a,b**) (**18a** being present only in small amounts) and $\{HB(3\text{-}^{i}Pr\text{-}4\text{-}Br\text{-}pz)_2(5\text{-}^{i}Pr\text{-}4\text{-}Br\text{-}pz)\}Rh(COD)$ (**15**).

being associated with five-coordinate forms, generally have the longer T_1 values than those of the corresponding COD compounds. It should be stressed here that, although, these values show the expected trend, they were obtained from fitting the data to single exponential decay, thus neglecting the presence of more than one isomer and the dynamics of their interconversion. More detailed relaxation studies would certainly be desirable.

5. Intramolecular Pyrazole Rearrangement. On one occasion the reaction of $[Tp^{iPr,4Br}]^-$ with $Rh_2Cl_2(COD)_2$, instead of giving $Tp^{iPr,4Br}Rh(COD)$ (**9**), gave an isomeric species which could be formulated as $\{HB(3\text{-}^{i}Pr\text{-}4\text{-}Br\text{-}pz)_2(4\text{-}Br\text{-}5\text{-}^{i}Pr\text{-}pz)\}$-Rh(COD) (**15**) with one of the pyrazolyl rings bonded to the boron atom through the nitrogen atom which, in the original ligand had been N^2 (i.e. this ring underwent an 1,2-shift at the nitrogen atoms). This assignment is based on a structural elucidation by means of a ^{103}Rh-^{1}H correlation and detailed two-dimensional NOE spectroscopy.

The ^{1}H-NMR spectrum was consistent with the presence of one COD unit and three pyrazolyl rings in the ratio of 2:1. However, their chemical shifts were different from those of the isomer **A** of **9**. The proton signals of **15** were related to a single ^{103}Rh resonance in the corresponding heteronuclear correlation, with chemical shifts, somewhat to higher field, but similar to those found for **9** suggesting that the former was an isomeric form of the latter. The presence of a 1,2-shifted pyrazolyl group was proven by the constraints implied by NOE methods. The low-field hydrogen resonance with unit integral (H^3 of the shifted ring), exhibited closeness to the olefinic protons of the COD moiety, whereas the broad BH resonance showed, in addition to those to the two equivalent H^5 protons, NOE to a unique isopropyl group, which in turn was found distant from the diene ligand. This latter constraint also implies that the 1,2-shifted pyrazolyl ring remains coordinated to rhodium, while the other two, from which one is free and the other coordinated, undergo rapid interchange on the NMR time scale. This observation is supported by the detection of a scalar coupling interaction between the ^{103}Rh spin and the H^3 proton of this unique ring as evidenced by the $^{103}Rh-^{1}H$ correlation experiment shown in Figure 5.

Table 5. ^{103}Rh Chemical Shifts of Pyrazolyl-Bridged Complexes of the Type $Rh_2(3R,4R,5R\text{-}pz)_2(COD)_2$[a]

3R	4R	5R	compd	ligating Ns	$\delta(^{103}Rh)$
Me	H	H	**16a**	N^1N^2	994
			16b	N^1N^1	966
				N^2N^2	1016
Me	Cl	Me	**17**	N^1N^1	1032
^{i}Pr	Br	H	**18a**	N^1N^2	1007
			18b	N^1N^1	969
				N^2N^2	1049

[a] Chemical shifts were measured indirectly in $CDCl_3$ by two-dimensional methods[9] and are expressed relative to the absolute scale $\Xi = 3.16$ MHz.

Heating a $CDCl_3$ solution of an authentic sample of $Tp^{iPr,4Br}$-Rh(COD) (**9**) to 70 °C for 30 min led to complete disappearance of signals due to the two isomeric forms of **9** while signals of the borotropic rearrangement product $\{HB(3\text{-}^{i}Pr\text{-}4\text{-}Br\text{-}pz)_2(5\text{-}^{i}Pr\text{-}4\text{-}Br\text{-}pz)Rh(COD)$ (**15**) emerged. This reaction is, however, accompanied by the formation of the sideproducts described in the next paragraph.

6. Decomposition Products. Although the complexes **4**–**14** were stable in $CDCl_3$ solutions for several days, on standing for longer time intervals they decomposed into products which proved to be dimeric complexes of the type shown for the Me^3-substituted pyrazolyl compound, **16**.

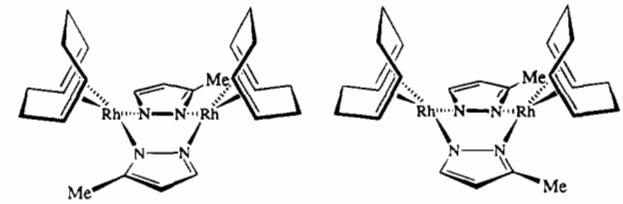

Complexes of this type were formed particularly easily from pyrazolylborates having halogen substituents in the 4-positions, i.e. $Rh_2\{3,5\text{-}Me_2\text{-}4\text{-}Cl\text{-}pz\}_2(COD)_2$ (**17**) and $Rh_2\{3\text{-}^{i}Pr\text{-}4\text{-}Br\text{-}pz\}_2(COD)_2$ (**18a,b**). The characterization of compounds **16**–**18** was achieved by one- and two-dimensional NMR spectroscopy. It should be noted that also compound **18** exists in two isomeric forms, depending on wether the two nitrogen atoms bonded to rhodium are of the same type (**b**) or not (**a**) (see Table 5). It is found that the C_s-symmetrical compound, i.e., that with two different rhodium environments, predominates in solution (see Figure 5). Pertinent ^{103}Rh NMR data are given in Table 5.

Analogous complexes with the NBD co-ligand were also observed, but were not further investigated as their study was complicated by additional dynamic processes.

Discussion

Crystal Structure. The X-ray crystal structure of $Tp^{Me}Rh$-(NBD) (**4**) shows that all three pyrazolyl rings are coordinated to the metal center, resulting in a distorted trigonal-bipyramidal coordination sphere for the rhodium. An earlier publication[4] showed a square-planar arrangement for the related complex pzTpRh(NBD) in which only two of the four pyrazolyl rings were coordinated to the metal. In the latter structure, the chelate adopts the usual boat conformation and the two non-coordinated pyrazolyl rings are found in pseudoaxial and pseudoequatorial positions. Depending on whether one or the other of these rings are substituted by H groups, the resulting structures can be taken as models for complexes of the type **A** or **B**, whereas the X-ray structure of **4** represents a model for compounds of type **C** (see Figure 2).

Solution Behavior. Solutions of the rhodium(I) complexes containing tris(pyrazolyl)borate ligands generally contained various isomeric species and showed dynamic behavior. The isomer distributions and interconversion rates were found to be influenced by (i) the substituents placed in the 3- and 5-positions of the pyrazolyl rings, (ii) the co-ligands attached to the rhodium center, and (iii) the polarity of the solvent employed. A discussion of the thermodynamic and kinetic aspects of this behavior is best carried out by considering the three low-energy structures presented in Figure 2, which shows two types of square-planar complexes (**A** and **B**) and one five-coordinate species. However, the trigonal-bipyramidal arrangement **C**, i.e., that found in **4**, should not be considered as static as, typically, five-coordinate complexes are fluxional. Indeed, the equivalence of the pyrazolyl rings in this form has been explained in terms of intramolecular exchange. Energy differences between the forms **A**, **B** and **C** are found to be small, as often two or more isomers can be detected simultaneously. The activation energies for the interconversion of these forms can be low, in particular for the exchange between complexes of types **B** and **C**. One can draw the following generalizations:

(i) Pyrazolyl Substituents. Large substituents in the 3-position of the pyrazolyl rings, e.g., ^{i}Pr, disfavor the formation of the five-coordinate species of type **C**. This is the case for the carbonyl complex $Tp^{iPr,4Br}Rh(CO)_2$ (**3**) which, as clearly shown by the IR spectroscopic studies, forms only the two four-coordinate isomers, **A** and **B**.

Two sets of resonances are also observed by ^{1}H and ^{13}C-NMR spectroscopy for complex **3** as well as the related compounds having the NBD or COD co-ligands, **6** and **9** respectively. The sets of resonances due to one of these compounds show the presence of inequivalent pyrazolyl rings in a 1:2 ratio and this species is assigned to structure **A** because of its symmetry. The second set, showing dynamically averaged pyrazolyl rings, is assigned a structure of type **B** because of the similarity of its ^{103}Rh chemical shift with that of the other isomer. There is *slow* intramolecular exchange at room temperature between these two forms, as shown by two-dimensional exchange spectroscopy and *rapid* intramolecular exchange of free and coordinated pyrazolyl ligands in the complex of type **B**. In this set of compounds, form **C** may be only a short-lived intermediate in this latter interconversion.

The presence of substituents in 5-position on the pyrazolyl rings considerably destabilizes form **A** due to steric repulsion between these two substituents on the two coordinated rings and the uncoordinated ring in the pseudoequatorial position. Consequently, the isomer of type **A** is no longer observed with ligands having this substitution pattern, e.g. in compounds **2**, **5**, **8**, and **10**−**13**. More generally, this is an extension of the tendency, already observed for the other tris(pyrazolyl) compounds, of the larger group to prefer to occupy a pseudoaxial position.

(ii) Co-ligands. The electronic nature and size of the co-ligands CO, NBD and COD influence the isomer distribution between forms **A**−**C**. Thus, with the exception of the complexes with unsubstituted pyrazolyl ligand, **14**, all the COD-containing complexes, **7**−**13**, can be assigned square-planar geometries, whereas the analogous NBD and CO derivatives can also form pentacoordinate isomers. Infrared and ^{1}H, ^{13}C, ^{15}N, and ^{103}Rh NMR spectroscopy for the carbonyl and diene complexes, respectively, proved invaluable for these assignments.

(iii) Solvent-Effect. The influence of the solvent on the isomer distribution was studied for the complexes $Tp^{iPr,4Br}Rh(CO)_2$ (**3**) and $Tp^{Me}Rh(CO)_2$ (**1**) by NMR and IR spectroscopy. While for **3** the IR study did not show the presence of a complex of type **C**, for **1** a change in solvent from $CHCl_3$ to MeCN caused a major shift of the equilibrium between forms **B** and **C** toward the five-coordinated complex of type **C**.

Variations in the coordination number in tris-pyrazolylborate complexes of Rh(I) are not limited to the solution phase, as can be seen from the few X-ray crystal structures reported for this class of compounds. In this respect one notes that Tp^{Me}-Rh(NBD) and pzTpRh(NBD) contain tri- and bidentate poly-(pyrazolyl)borates, respectively, although from considerations of steric demands of the ligands, the opposite would be expected.[11]

The above study clearly shows that a thorough study of the solution behavior of complexes of the type $Tp^{3R,4R,5R}Rh(LL)$ is required before structural assignments can be made.

Decomposition Products and Borotropic Migration. In addition to the structural considerations mentioned earlier, the observation of decomposition products is worthy of comment: The formation of complexes of the type $Rh_2(3R,4R,5R\text{-pz})_2(COD)_2$ implies the cleavage of B−N bonds. This could occur either by electrophilic attack of a proton at the uncoordinated nitrogen atom or nucleophilic attack at boron, e.g. by OH^-. The formation of the borotropic migration product {HB(3-^{i}Pr-4-Br-pz)$_2$(5-^{i}Pr-4-Br-pz)}Rh(COD) (**15**), can be induced thermally, and might also be related to these processes as it is accompanied by the formation of corresponding sideproducts.

It is interesting to note that there appears to be a correlation between the rate of decomposition and the presence of isomers of type **A**. Thus, the pyrazole-bridged dimeric complex Rh_2(3-^{i}Pr-4-Br-pz)$_2$(COD)$_2$ (**18**) is formed within a few hours in $CDCl_3$ solution, from $Tp^{iPr,4Br}Rh(COD)$ (**9**) which exists to *ca.* 75% in the form of isomer **A**. Its borotropic rearrangement product Rh{HB(3-^{i}Pr-4-Br-pz)$_2$(5-^{i}Pr-4-Br-pz)}(COD) (**15**), existing as the isomer of type **B**, seems to be more robust, showing a slower decomposition rate. Whereas nitrogen protonation seems equally likely for both conformations, nucleophilic attack at the boron atom, or at the BH bond, however, could occur more easily in the isomer of type **A**, where the boron atom is more exposed.

Experimental Section

Analytical Measurements. C, H, and N analyses were performed by the Mikroelementaranalytisches Laboratorium der Eidgenössischen Technischen Hochschule Zürich.

Infrared Spectroscopy. Spectra were recorded in RbI pellets or as $CHCl_3$ and MeCN solutions in NaCl cells on a Perkin-Elmer Model 883 spectrophotometer.

NMR Spectroscopy. One-dimensional ^{1}H, ^{13}C, and ^{11}B and two-dimensional NOESY and HMQC (^{13}C,^{1}H; ^{15}N,^{1}H and ^{103}Rh,^{1}H) NMR spectra were recorded on Bruker AMX 500, AC 250, and AC 200 spectrometers. The chemical shift scales are relative to internal TMS (^{1}H and ^{13}C), external BF_3·Et_2O (^{11}B), external $MeNO_2$ (^{15}N) and Ξ = 3.16 MHz (^{103}Rh).

Materials. Pyrazole and 3,5-dimethylpyrazole, purchased from Fluka AG, and 3-methylpyrazole, obtained from Merck AG, were used without further purification. 3,4,5-Trimethylpyrazole, 3,5-dimethyl-4-chloropyrazole, 3(5)-methyl-5(3)-phenylpyrazole and 3(5)-trifluoromethyl-5(3)-methylpyrazole were synthesized from the corresponding β-diketone (purchased from Fluka AG or Merck AG) with hydrazine hydrate (NH_2NH_2·H_2O) obtained from Merck AG.[12,13] 1,1,1-Trifluoro-

(11) It had been pointed out by a reviewer that the fourth pyrazolyl ligand in the complex pzTpRh(NBD) could lead to interference with the H-5 hydrogens and favor a bidentate coordination in this compound. See, e.g., also: Sohrin, Y.; Kokusen, H.; Kihara, S.; Matsui, M.; Kushi, Y.; Shiro, M. *J. Am. Chem. Soc.* **1993**, *115*, 4128.
(12) Chambers, D.; Denny, W. *J. Org. Chem.* **1985**, *50*, 4736.
(13) Nishiwaki, T. *J. Chem. Soc. B* **1967**, 885.

2,4-pentadione and 4-chloro-2,4-pentadione were distilled before use, whereas the others were used as obtained. K[Tp^{iPr,4Br}] was kindly provided by S. Trofimenko. The organometallic starting materials [$Rh_2Cl_2(CO)_4$],[14] [$Rh_2Cl_2(COD)_2$],[15] and [$Rh_2Cl_2(NBD)_2$],[16] were prepared as described in the appropriate references. The complexes {$Ph_2B(pz)_2$}Rh(LL),[10] {$BBN(pz)_2$}Rh(LL),[10] {$BBN(3\text{-Me-}pz)_2$}Rh(LL),[10] {PhMeB(3-Me-pz)$_2$}Rh(LL),[8] and {$MeB(3\text{-Me-}pz)_3$}Rh(LL)[8] were available from other studies.

Sodium Tris(pyrazolylborates), General Procedure. $NaBH_4$ (0.1 mol) and the appropriate pyrazole (0.5 mol) were suspended in ca. 130 mL of kerosene. The reaction mixture was heated slowly in an oil bath to 220 °C (<200 °C for pyrazoles with 5R = H to avoid the formation of tetrakis(pyrazolyl)borates), while monitoring the amount of evolved hydrogen gas. The reaction was halted at the stage where 3 equiv of H_2 had evolved and the reaction mixture was then allowed to cool to ca. 180 °C. The product, in the form of white microcrystals, was removed by filtration, repeatedly washed with petroleum ether and dried under HV.

Na[Tp]: Yield: 68%. Anal. Found (calcd for $C_9H_{10}BN_6Na$): C 45.80 (45.37); H 4.27 (4.11); N 35.61 (36.16). ^{1}H-NMR (D_2O): 7.65 (d, H^3); 7.38 (d, H^5); 6.32 (dd, H^4). ^{13}C-NMR (D_2O): 143.5 (C^3); 137.2 (C^5); 107.5 (C^4). ^{11}B-NMR (acetone-d_6): −4.6.

Na[Tp^{Me}]: Yield: 86%. Anal. Found (calcd for $C_{12}H_{16}BN_6Na$): C 51.29 (51.86); H 6.62 (5.80); N 30.66 (30.22). ^{1}H-NMR (CD_3CN): 7.47 (d, H^5); 5.83 (d, H^4); 2.24 (s, Me^3). ^{13}C-NMR (CD_3CN): 149.5 (C^3); 136.3 (C^5); 103.4 (C^4); 13.8 (Me^3). ^{11}B-NMR (CD_3CN): −4.9.

Na[Tp^{Me2}]: Yield: 61%. Anal. Found (calcd for $C_{15}H_{22}BN_6Na$): C 56.44 (56.27); H 6.86 (6.93); N 26.05 (26.25). ^{1}H-NMR (CD_3CN): 5.57 (s, H^4); 2.29, 2.13 (Me^3, Me^5). ^{13}C-NMR (CD_3CN): 148.2 (C^3); 144.6 (C^5); 118.7 (C^4); 14.2, 13.8 (Me^3, Me^5). ^{11}B-NMR (acetone-d_6): −11.4.

Na[Tp^{Me3}]: Yield: 51%. Anal. Found (calcd for $C_{18}H_{28}BN_6Na$): C 58.94 (59.68); H 7.89 (7.79); N 23.56 (23.20). ^{1}H-NMR ($CDCl_3$): 2.28, 2.08, 1.89 (3Me). ^{13}C-NMR ($CDCl_3$): 146.8 (C^3); 141.9 (C^5); 110.3 (C^4); 12.5, 11.6, 8.3 (3Me). ^{11}B-NMR ($CDCl_3$): −11.1.

Na[Tp^{Me2,4Cl}]: Yield: 67%. Anal. Found (calcd for $C_{15}H_{19}BCl_3N_6Na$): C 42.00 (42.54); H 4.45 (4.52); N 19.82 (19.84); Cl 24.85 (25.11). ^{1}H-NMR ($CDCl_3$): 2.30, 2.01 (2Me). ^{13}C-NMR ($CDCl_3$): 145.3 (C^3); 140.9 (C^5); 107.3 (C^4); 11.5, 10.9 (2Me). ^{11}B-NMR ($CDCl_3$): −7.9.

Na[Tp^{CF3,Me}]: Yield 58%. Anal. Found (calcd for $C_{15}H_{13}BF_3N_6Na$): C 36.98 (37.37); H 2.89 (2.72); N 17.05 (17.43); F 35.70 (35.46). ^{1}H-NMR ($CDCl_3$): 6.17 (s, H^4), 2.44 (s, Me^5). ^{13}C-NMR (acetone-d_6): 146.5 (C^5); 142.6 (q, $J_{F,C}$ = 36.2 Hz, C^3); 123.3 (q, $J_{F,C}$ = 267.2 Hz, CF_3); 103.7 (q, $J_{F,C}$ = 1.9 Hz, C^4); 13.0 (Me^5). ^{11}B-NMR (acetone-d_6): −7.9. ^{19}F-NMR ($CDCl_3$): −62.2.

Na[Tp^{Ph,Me}]: Yield: 57%. Anal. Found (calcd for $C_{30}H_{28}BN_6Na$): C 70.98 (71.16); H 5.72 (5.57); N 16.45 (16.60). ^{1}H-NMR ($CDCl_3$): 7.46 (m, H^o); 7.28−7.13 (m, H^m, H^p); 6.20 (s, H^4); 2.21 (s, Me^5). ^{13}C-NMR (acetone-d_6): 151.8 (C^3); 145.4 (C^5); 136.4 (C^i); 129.4 (C^o); 127.2 (C^p); 126.5 (C^m); 103.2 (C^4); 13.4 (Me^5). ^{11}B-NMR (acetone-d_6): −5.5.

Rhodium(I) Complexes, General Procedure. To a solution of the appropriate Rh_2Cl_2(LL) (LL = 2 CO, NBD, COD) compound (150 mg in 10 mL of MeCN), at −20 °C, two equivalents of the solid pyrazolylborate ligands were added at once. The mixture was stirred for 1 h while the temperature was allowed to rise to 25 °C. The solvent was then removed under vacuum, the residue was extracted with 50 mL of hexane and the extract filtered through Celite to remove MCl (M = Na, K). After evaporation of hexane under vacuum, the resulting product was recrystallized by careful addition of MeCN to a CH_2Cl_2 solution and storage at −20 °C for 20 h. Yields, analytical and spectroscopic data are as follows:

Tp^{Me}Rh(CO)$_2$, 1: Yield: 56%. Anal. Found (calcd for $C_{14}H_{16}BN_6O_2Rh$): C 40.27 (40.61); H 3.97 (3.90); N 20.09 (20.30). ^{1}H-NMR: 7.48 (br, 3H, H^5); 6.00 (d, 3H, H^4); 2.44 (s, 9H, Me^3). ^{13}C-NMR: 150.7 (C^3); 136.1 (C^5); 105.1 (C^4); 15.1 (Me^3).

Tp^{Me2}Rh(CO)$_2$, 2: Yield: 53%. Anal. Found (calcd for $C_{17}H_{22}BN_6O_2Rh$): C 43.23 (44.77); H 4.79 (4.86); N 17.73 (18.43). ^{1}H-NMR: 5.98 (s, 3H, H^4); 2.38, 2.33 (s, 2 × 9H, Me^3, Me^5). ^{13}C-NMR: 149.6 (C^3); 144.4 (C^5); 105.9 (C^4); 15.2, 12.7 (Me^3, Me^5).

Tp^{iPr,4Br}Rh(CO)$_2$, 3: Yield: 47%. Anal. Found (calcd for $C_{20}H_{25}BBr_3N_6O_2Rh$): C 32.57 (32.69); H 3.52 (3.43); N 11.59 (11.44). ^{1}H-NMR: isomer A, 7.70 (s, 1H, H$^{5'}$); 7.28 (s, 2H, H^5); 3.34 (sept, 2H, ^{i}Pr); 3.17 (sept, 1H, ^{i}Pr′); 1.45, 1.30 (2d, 3 × 6H, ^{i}Pr); 1.37 (d, 6H, ^{i}Pr′); isomer B, 7.54 (s, 3H, H^5); 3.41 (sept, 3H, ^{i}Pr); 1.37 (d, 18H, ^{i}Pr). ^{13}C-NMR: isomer A, 159.0 (1C, C$^{3'}$); 156.5 (2C, C^3); 137.6 (2C, C^5); 137.2 (1C, C$^{5'}$); 92.4 (1C, C$^{4'}$); 90.9 (2C, C^4); 30.8, 21.9, 20.1 (3 × 2C, ^{i}Pr); 26.9, 20.7 (1C, 2C, ^{i}Pr′); isomer B, 156.8 (C^3); 138.3 (C^5); 91.2 (C^4); 30.0, 20.7 (^{i}Pr).

Tp^{Me}Rh(NBD), 4: Yield: 74%. Anal. Found (calcd for $C_{19}H_{24}BN_6Rh$): C 50.67 (50.70); H 5.42 (5.37); N 19.72 (18.67). ^{1}H-NMR: 7.45 (s, br, 3H, H^5); 5.96 (d, 3H, H^4); 4.27 (q, br, 1H, BH); 3.75 (m, 4H, H^{ol}); 3.68 (m, 2H, H^{brh}); 2.51 (s, 9H, Me^3); 1.17 (m, 2H, H^{br}). ^{13}C-NMR: 151.2 (C^3); 135.6 (C^5); 105.5 (C^4); 59.5 (C^{br}) J(Rh,C) = 6.6 Hz; 48.9 (C^{brh}) J(Rh,C) = 2.5 Hz; 41.9 (br, C^{ol}); 14.7 (Me^3). ^{13}C-NMR (solid state): 152 (C^3); 136 (C^5); 107 (C^4); *ca.* 58 (C^{br}); *ca.* 49 (C^{brh}); 30−35 (C^{ol}).

Tp^{Me2}Rh(NBD), 5: Yield: 72%. Anal. Found (calcd for $C_{22}H_{30}BN_6Rh$): C 53.52 (53.68); H 6.20 (6.14); N 16.93 (17.08). ^{1}H-NMR: 5.71 (s, 3H, H^4); 4.42 (q, br, 1H, BH); 3.66 (m, 2H, H^{brh}); 3.58 (m, 4H, H^{ol}); 2.50, 2.26 (2s, 2 × 9H, Me^3, Me^5); 1.15 (m, 2H, H^{br}). ^{13}C-NMR: 150.6 (C^3); 143.6 (C^5); 106.7 (C^4); 58.1 (C^{br}); 48.1 (C^{brh}); 35.1 (C^{ol}); 14.9, 12.9 (Me^3, Me^5).

Tp^{iPr,4Br}Rh(NBD), 6: Yield: 68%. Anal. Found (calcd for $C_{25}H_{33}BN_6Rh$): C 38.41 (38.95); H 4.23 (4.31); N 10.66 (10.90). ^{1}H-NMR: isomer A, 7.90 (s, 1H, H$^{5'}$); 7.13 (s, 2H, H^5); 5.9 (vbr, 1H, BH); 4.14 (m, br, 4H, H^{ol}); 3.98 (m, br, 2H, H^{brh}); 3.29, 1.37, 1.25 (sept, 2d, 2H, 2 × 6H, ^{i}Pr); 3.17, 1.31 (sept, d, 1H, 6H, ^{i}Pr′); isomer B, 7.60 (s, 3H, H^5); 4.3 (vbr, 1H, BH); 3.77 (m, 4H, H^{ol}); 3.59 (m, 2H, H^{brh}); 3.31, 1.33 (sept, d, 3H, 18H, ^{i}Pr); 1.13 (m, 2H, H^{br}). ^{13}C-NMR: isomer A, 158.3 (1C, C$^{3'}$); 155.5 (2C, C^3); 137.5 (1C, C$^{5'}$); 136.5 (2C, C^5); 91.9 (1C, C$^{4'}$); 89.7 (2C, C^4); 62.7 (1C, C^{br}); *ca.* 57 (vbr, C^{ol}); 50.8 (2C, C^{brh}); 29.1, 26.9, 21.9, 21.1, 20.6 (^{i}Pr + ^{i}Pr′); isomer B, 156.6 (C^3); 138.1 (C^5); 90.3 (C^4); 62.7 (C^{br}) J(Rh,C) = 6.1; 57.7 (C^{ol}) J(Rh,C) = 9.7; 50.6 (C^{brh}) J(Rh,C) = 2.0; 29.0, 21.0 (^{i}Pr).

Tp^{Me}Rh(COD), 7: Yield: 62%. Anal. Found (calcd for $C_{20}H_{28}BN_6Rh$): C 51.30 (51.53); H 6.02 (6.05); N 17.89 (18.03). ^{1}H-NMR: isomer A, 7.81 (d, 1H, H$^{5'}$); 7.20 (d, 2H, H^5); 6.13 (br, 1H, H$^{4'}$); 6.1 (vbr, 1H, BH); 5.81 (d, 2H, H^4); 4.13 (m, 4H, H^{ol}); 2.51 (m, 4H, H^{exo}); 2.38 (s, 3H, Me$^{3'}$); 2.36 (s, 6H, Me^3); 1.86 (m, 4H, H^{endo}); isomer B, 7.54 (d, 3H, H^5); 6.03 (d, 3H, H^4); 4.35 (vbr, 1H, BH); 4.12 (m, 4H, H^{ol}); 2.40 (s, 9H, Me^3); 2.14 (m, 4H, H^{exo}); 1.59 (m, 4H, H^{endo}). ^{13}C-NMR: isomer B, 151.2 (C^3); 135.6 (C^5); 105.5 (C^4); 79.7 (C^{ol}), J(Rh,C) = 12.6 Hz; 29.9 (CH_2); 14.7 (Me^3).

Tp^{Me2}Rh(COD), 8: Yield: 65%. Anal. Found (calcd for $C_{23}H_{34}BN_6Rh$): C 53.97 (54.35); H 6.75 (6.74); N 16.60 (16.53). ^{1}H-NMR: 5.81 (s, 3H, H^4); 4.44 (vbr, 1H, BH); 4.13 (m, 4H, H^{ol}); 2.34, 2.13 (2s, 2 × 9H, Me^3, Me^5); 2.13 (m, 4H, H^{exo}); 1.59 (m, 4H, H^{endo}). ^{13}C-NMR: 150.6 (C^3); 143.6 (C^5); 106.7 (C^4); 75.2 (C^{ol}), J(Rh,C) = 12.4; 26.2 (CH_2); 14.9, 12.9 (Me^3, Me^5).

Tp^{iPr,4Br}Rh(COD), 9: Yield: 60%. Anal. Found (calcd for $C_{26}H_{37}BBrN_6Rh$): C 39.22 (39.68); H 4.79 (4.74); N 9.54 (9.68). ^{1}H-NMR: isomer A, 7.88 (s, 1H, H$^{5'}$); 7.24 (s, 2H, H^5); 6.25 (vbr, 1H, BH); 4.20, 4.17 (2m, 2 × 2H, H^{ol}); 3.39, 3.33, 3.16, 1.36, 1.34, 1.22 (3 sept, 3d,

Table 6. Crystallographic Data for Tp^{Me}Rh(NBD) (4)

formula	$C_{19}H_{24}N_6BRh$	Z	8
mol wt	450.16	ϱ_{calcd}, g cm^{-3}	1.54
cryst syst	monoclinic	μ, cm^{-1}	8.02
space group	$P2_1/c$ (No. 14)	λ, Å	0.710 69 (graphite monochromated, Mo Kα)
a, Å	18.152(3)		
b, Å	16.732(4)	T, °C	25
c, Å	20.591(4)	R^a	0.0457
β, deg	141.793(7)	R_w^b	0.0412
V, Å^3	3867.9		

^{a} $R = \sum||F_o| - |F_c||/\sum|F_o|$. ^{b} $R_w = \sum w^{1/2}\,|(|F_o| - |F_c|)|/\sum w^{1/2}|F_o|$, $w = k/\sigma^2(F_o)$, k = 2.01.

(14) McCleverty, J. A.; Wilkinson, G. *Inorg. Synth.* **1966**, *8*, 211.
(15) Chatt, J.; Venanzi, L. M. *J. Chem. Soc.* **1957**, 4735.
(16) Abel, E. W.; Bennett, M. A.; Wilkinson, G. *J. Chem. Soc.* **1959**, 3178.

Table 7. Final Positional Parameters and Equivalent Thermal Parameters (pm^2) for $Tp^{Me}Rh(NBD)$ (**4**)

atom	*x*	*y*	*z*	$U_{iso/eq}$	atom	*x*	*y*	*z*	$U_{iso/eq}$
Rh1	0.06778(5)	0.20883(5)	0.14425(5)	320(6)	Rh2	0.41457(5)	0.20475(5)	0.08733(5)	317(6)
B1	0.043(1)	0.4008(7)	0.1353(9)	430(116)	B2	0.465(1)	0.3958(7)	0.135(1)	500(130)
H1	0.042(8)	0.469(6)	0.141(7)	800	H2	0.469(8)	0.461(6)	0.142(7)	800
N11a	0.1986(5)	0.3051(5)	0.2083(5)	371(62)	N11b	0.2961(5)	0.3031(5)	0.0406(5)	383(62)
N12a	0.1701(6)	0.3813(5)	0.2051(6)	430(79)	N12b	0.3339(6)	0.3807(5)	0.0606(6)	503(88)
C11a	0.2556(9)	0.4310(6)	0.2452(7)	641(108)	C11b	0.2535(9)	0.4308(6)	0.0317(8)	670(125)
C12a	0.3418(9)	0.3873(8)	0.2737(7)	677(109)	C12b	0.1623(9)	0.3867(7)	−0.0085(8)	641(113)
C13a	0.3042(7)	0.3086(7)	0.2500(6)	485(86)	C13b	0.1907(7)	0.3060(6)	0.0003(6)	444(85)
C14a	0.3606(8)	0.2361(7)	0.2586(7)	589(97)	C14b	0.1270(8)	0.2337(6)	−0.0222(7)	523(92)
N21a	−0.0514(5)	0.2830(4)	0.0068(5)	315(59)	N21b	0.5391(6)	0.2627(5)	0.2362(6)	369(71)
N22a	−0.0404(6)	0.3651(4)	0.0245(5)	357(69)	N22b	0.5406(6)	0.3449(5)	0.2342(6)	424(82)
C21a	−0.1127(7)	0.4057(6)	−0.0656(7)	486(100)	C21b	0.6199(8)	0.3733(7)	0.3316(7)	529(109)
C22a	−0.1719(8)	0.3500(6)	−0.1443(7)	485(99)	C22b	0.6696(8)	0.3095(7)	0.3991(7)	542(99)
C23a	−0.1324(7)	0.2743(6)	−0.0970(6)	373(78)	C23b	0.6191(7)	0.2410(6)	0.3388(6)	392(81)
C24a	−0.1712(7)	0.1955(6)	−0.1496(7)	474(90)	C24b	0.6420(8)	0.1566(6)	0.3736(7)	554(103)
N31a	0.0023(5)	0.2849(5)	0.1815(5)	401(64)	N31b	0.4936(5)	0.2904(6)	0.0687(5)	422(64)
N32a	0.0041(6)	0.3670(5)	0.1736(6)	466(85)	N32b	0.4936(6)	0.3696(5)	0.0846(6)	485(84)
C31a	−0.0518(9)	0.4032(7)	0.1846(7)	607(110)	C31b	0.5471(9)	0.4127(8)	0.0755(7)	660(119)
C32a	−0.0925(9)	0.3447(8)	0.1976(8)	656(114)	C32b	0.5806(9)	0.3616(9)	0.0518(8)	715(126)
C33a	−0.0560(8)	0.2727(7)	0.1966(6)	479(88)	C33b	0.5493(7)	0.2850(8)	0.0495(6)	501(81)
C34a	−0.0829(8)	0.1903(8)	0.2049(7)	646(103)	C34b	0.5774(8)	0.2064(9)	0.0386(7)	626(100)
C41a	−0.0151(9)	0.0982(6)	0.0826(8)	513(112)	C41b	0.4795(9)	0.0889(6)	0.1272(7)	458(103)
C42a	0.0708(8)	0.1049(6)	0.0899(7)	545(114)	C42b	0.3916(9)	0.0924(6)	0.1152(8)	518(127)
C43a	0.1867(9)	0.0669(6)	0.1986(9)	625(131)	C43b	0.2757(9)	0.0691(6)	0.0026(8)	578(129)
C44a	0.2148(8)	0.1307(6)	0.2682(7)	517(104)	C44b	0.2578(8)	0.1423(6)	−0.0528(7)	452(96)
C45a	0.1329(8)	0.1242(6)	0.2604(7)	500(113)	C45b	0.3422(8)	0.1379(6)	−0.0436(7)	467(103)
C46a	0.0476(9)	0.0562(6)	0.1823(8)	639(130)	C46b	0.4148(9)	0.0619(6)	0.0201(8)	590(125)
C47a	0.136(1)	0.0011(7)	0.2072(9)	779(144)	C47b	0.318(1)	0.0077(6)	−0.0199(8)	674(138)

3 × 1H, 3 × 6H, ^{i}Pr); 2.54 (m, 4H, H^{exo}); 1.86 (m, 4H, H^{endo}); isomer B, 7.61 (s, 3H, H^5); 4.15 (vbr, 1H, BH); 3.96 (m, 4H, H^{ol}); 3.33, 1.33 (sept, d, 3H, 18H, ^{i}Pr); 2.15 (m, 4H, H^{exo}); 1.61 (m, 4H, H^{endo}). ^{13}C-NMR: isomer A, 158.3 (1C, $C^{3'}$); 155.2 (2C, C^3); 138.3 (1C, $C^{5'}$); 137.0 (2C, C^5); 91.8 (1C, $C^{4'}$); 90.0 (2C, C^4); 84.2, 78.0 (2 × 2C, C^{ol}); 30.3 (4C, CH_2^{COD}); 29.4, 27.0, 21.9, 21.0, 20.9 (^{i}Pr); isomer B, 156.9 (C^3); 138.9 (C^5); 90.8 (C^4); 81.6 (C^{ol}); 29.6 (CH_2^{COD}); 29.2, 21.1 (^{i}Pr).

Tp^{Me3}Rh(COD), 10: ^{1}H-NMR: 4.5 (vbr, 1H, BH); 4.08 (m, 4H, H^{ol}); 2.04 (m, 4H, H^{exo}); 1.57 (m, 4H, H^{endo}); 2.28, 2.05, 1.88 (3s, 3 × 9H, Me^{3-5}).

$Tp^{Me2,4Cl}$Rh(COD), 11: ^{1}H-NMR: 4.4 (vbr, 1H, BH); 4.10 (m, 4H, H^{ol}); 2.09 (m, 4H, H^{exo}); 1.63 (m, 4H, H^{endo}); 2.34, 2.14 (2s, 2 × 9H, Me^3, Me^5).

$Tp^{Ph,Me}$Rh(COD), 12: ^{1}H-NMR: 8.03 (d,br, 6H, H^o); 7.47 (t, 6H, H^m); 7.37 (t, 3H, H^p); 6.29 (s, 3H, H^4); 4.8 (vbr, 1H, BH); 3.33 (m, 4H, H^{ol}); 2.34 (s, 9H, Me^5); 1.61 (m, 4H, H^{exo}); 1.09 (m, 4H, H^{endo}).

$Tp^{CF3,Me}$Rh(COD), 13: ^{1}H-NMR: 6.39 (s, 3H, H^4); 4.6 (vbr, 1H, BH); 4.13 (m, 4H, H^{ol}); 2.27 (s, 9H, Me^5); 2.04 (m, 4H, H^{exo}); 1.58 (m, 4H, H^{endo}).

TpRh(COD), 14: ^{1}H-NMR: 7.76, 7.58 (2d, 2 × 3H, $H^{3,5}$); 6.21 (t, 3H, H^4); 4.45 (q, vbr, 1H, BH); 3.95 (m, 4H, H^{ol}); 2.58 (m, 4H, H^{exo}); 1.90 (m, 4H, H^{endo}). ^{13}C-NMR: 139.4 (C^3); 134.8 (C^5); 104.7 (C^4); 73.3 (C^{ol}) J(Rh,C) = 13.7 Hz; 31.2 (CH_2^{COD}).

{HB(3-^{i}Pr-4-Br-pz)$_2$(4′-Br-5′-^{i}Pr-pz)}Rh(COD), 15: ^{1}H-NMR: 7.45 (s, 2H, H^5); 7.14 (s, 1H, $H^{3'}$); 4.4 (vbr, 1H, BH); 3.92 (m, 4H, H^{ol}); 2.17 (m, 4H, H^{exo}); 1.65 (m, 4H, H^{endo}); 3.46, 1.38, 1.35 (sept, d, d, 2H, 2 × 6H, ^{i}Pr); 3.59, 1.33 (sept, d, 1H, 6H, ^{i}Pr′).

Rh_2{3-Me-pz)$_2$(COD)$_2$, 16: ^{1}H-NMR: isomer a, 7.07 (d, 2H, H^5); 5.74 (d, 2H, H^4); 4.46, 4.27, 4.12, 4.01 (4 × m, 4 × 2H, H^{ol}); 2.87, 2.80, 2.73, 2.59 (4 × m, 4 × 2H, H^{exo}); 2.42 (s, 6H, Me^3); 2.10, 2.02 (2 × m, 2 × 4H, H^{endo}); isomer b, 7.19 (d, 2H, H^5); 5.74 (d, 2H, H^4); 4.31, 4.30, 4.17 (4 × m, 4 × 2H, H^{ol}); 2.87, 2.80, 2.65, 2.60 (4 × m, 4 × 2H, H^{exo}); 2.39 (s, 6H, Me^3); 2.09, 1.99 (2 × m, 2 × 4H, H^{endo}).

Rh_2{3,5-Me_2-4-Cl-pz}$_2$(COD)$_2$, 17: ^{1}H-NMR: 4.46, 4.31 (2m, 2 × 2H, H^{ol}); 2.85, 2.60 (2m, 2 × 2H, H^{exo}).

Rh_2{3-^{i}Pr-4-Br-pz}$_2$(COD)$_2$, 18: ^{1}H-NMR: isomer a, 7.04 (s, 2H, H^5); 3.70, 1.35, 1.06 (sept, d, d, 2H, 2 × 6H, ^{i}Pr); 4.45, 4.35, 4.12, 3.96 (4m, 4 × 2H, H^{ol}); 2.8, 2.6, 2.48 (4m, 2 × 2H, 4H, H^{exo}); 2.1, 2.0 (2m, 2 × 4H, H^{endo}); isomer b, 7.19 (s, 2H, H^5); 3.59, 1.31, 1.22 (sept, d, d, 2H, 2 × 6H, ^{i}Pr); 4.27, 4.19, 4.17, 4.10 (4m, 4 × 2H, H^{ol}); 2.89, 2.74, 2.60, 2.58 (4m, 4 × 2H, H^{exo}); 2.08, 1.98 (2m, 2 × 4H, H^{endo}).

Crystallography. Air-stable yellow crystals of $Tp^{Me}Rh(NBD)$ (**4**), suitable for X-ray diffraction, were obtained by crystallization from toluene. Crystallographic data were collected on a STOE 4-circle diffractometer STADI 4 using the $\omega/2\theta$ scan technique and learned profile method. An empirical absorption correction, based on a series of Ψ scans, as well as Lorentz and polarization corrections were applied. A list of crystallographic and other relevant data is given in Table 6. All hydrogen atom positions, except for H1, were placed in calculated positions with fixed isotropic temperature displacement parameters (800 pm^2). Anisotropic temperature factors were used for all non-hydrogen atoms. Final atomic coordinates for the two crystallographically independent molecules in the asymmetric unit and equivalent thermal parameters for the heavy atoms are given in Table 7.

Acknowledgment. U.E.B. carried out the work during the tenure of a grant from the Research Commission of the ETH Zürich. A.C. thanks the Swiss National Science Foundation for support. The authors are indebted to Dr. S. Trofimenko for providing a sample of Na[$Tp^{iPr,4Br}$].

Supplementary Material Available: Text detailing the structure refinement and tables of anisotropic displacement parameters for the two crystallographically independent molecules in the asymmetric unit (Table S1), hydrogen positions (Table S2), an extended list of bond distance and angles (Table S3) for **4**, and full experimental details of the structure solution (Table S4) (8 pages). Ordering information is given on any current masthead page.